

Silicon MEMS for Photonic Bandgap Devices

E.M. Yeatman and A. Lipson

Department of Electrical & Electronic Engineering
Imperial College London
Exhibition Rd., London SW7 2AZ, U.K.
e.yeatman@imperial.ac.uk, a.lipson@imperial.ac.uk

ABSTRACT

An optical filter is presented based on lateral beam propagation between input and output fibers, through a 1-dimensional silicon photonic bandgap (PBG) structure. Optical modelling of the device shows that a very high degree of verticality is needed for the PBG surfaces, and a fabrication technique is described by which these can be obtained, using a combination of wet and dry silicon etching steps.

Keywords: optical filter, anisotropic etching, photonic bandgap

1 INTRODUCTION

Photonic Bandgap (PBG) devices have been widely investigated in recent years because of their capabilities for manipulating light within highly constrained dimensions. These capabilities arise from the characteristic structure of PBG devices, which combines periodicity with high refractive index contrast. The periodicity can be in 1, 2 or 3 dimensions; although only a 3-D periodic structure can exhibit a true photonic bandgap in analogy with the electronic bandgap of semiconductors, most reported devices have been 1-D or 2-D because of fabrication constraints. Even with this restriction, the resonant nature of PBG devices demands high structural precision and surface quality if the desired optical performance is to be achieved.

Many PBG devices have been fabricated in III-V semiconductors in order to take advantage of the active optoelectronic properties of these materials. Generally the PBG structure is a 2-D pattern etched down from the surface, with the semiconductor-air interfaces providing the refractive index contrast. However, high excess scattering losses, because of the poor surface quality, have typically resulted in device insertion losses unacceptably high for useful devices. For this reason we have explored silicon as an alternative PBG material. Far higher etched surface quality is achievable in silicon as a result of the initial quality of the crystalline material, and the better etch processes available compared to compound semiconductors, both for dry and wet etching. Although silicon does not offer active optoelectronic properties, combining PBG with MEMS actuators allows functionality

such as wavelength tuning to be incorporated. This opens opportunities for optical processing and sensing applications, such as spectrometry.

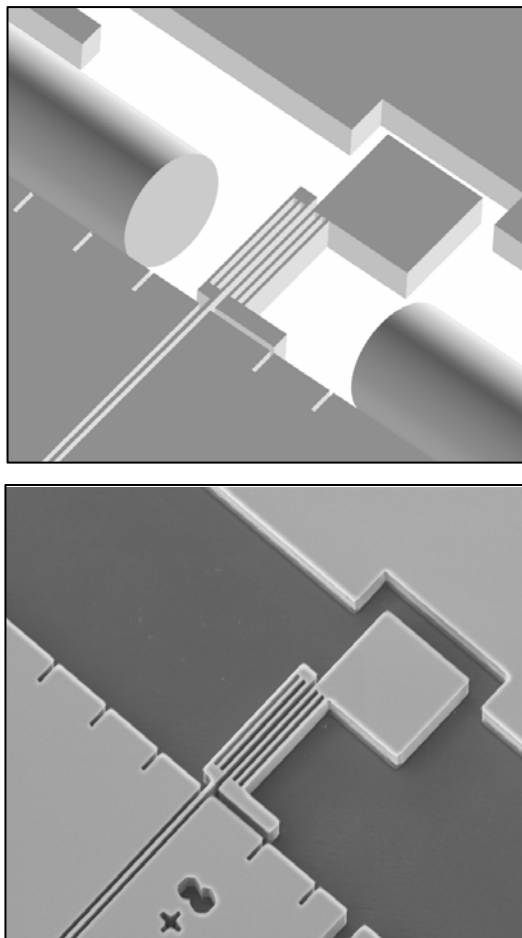


Figure 1: 3D schematic of device with fibers inserted (top), and electron micrograph of fabricated filter structure (bottom).

The devices we have fabricated are wavelength filters which use 1-D PBG cavities, so that the crucial interfaces are planar, as illustrated in Fig. 1. Other devices of this sort have been previously fabricated, using dielectric stacks, but these suffer from more complicated packaging and alignment, or smaller stop bands, and have limited

integration potential [1-3]. If silicon is used, only three silicon-air paired layers are needed for each mirror, making the device extremely compact and potentially low loss. An in-plane design, where the PBG structure is etched into the substrate and the fibers are incorporated in-plane, eases the integration process and allows construction of a high quality filter with easy to fit grooves and springs for the fibers.

Deep reactive ion etching (DRIE) allows projection of the photolithographic device pattern into the substrate with high aspect ratio and good sidewall angle. However, the resulting surfaces are still insufficiently flat and vertical to give the desired performance. By using (110) oriented wafers with vertical (111) planes, we follow the DRIE step with a short anisotropic wet chemical etch, polishing the

critical (111) surfaces to atomic precision, and ensuring both the flatness and verticality required.

2 DEVICE DESIGN AND MODELLING

In order for the device to have good optical properties, the PBG structure must be extremely vertical, accurate in dimensions, and have optically smooth surfaces. For a fiber-to-fiber, free-space design, where a relatively wide beam is needed and consequently a high aspect ratio structure, non-vertical structures change the optical thickness the light beam encounters from top to bottom. This consequentially widens the pass band and increases the loss.

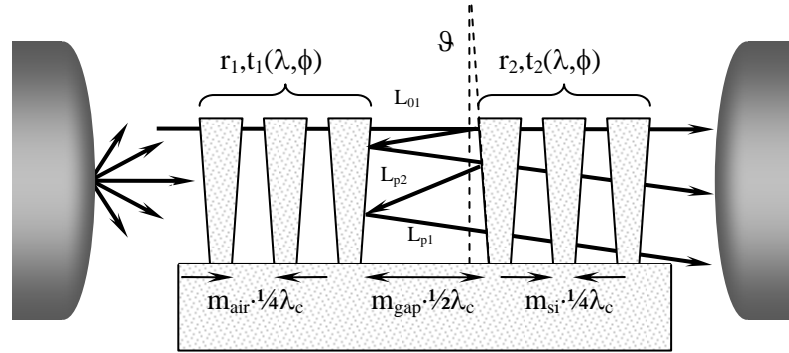


Figure 2: Geometry and labeling conventions used for filter analysis.

Fig. 2 shows the cross section of the device. The 1D PBG filter is made up of alternating silicon and air layers, each a quarter of a wavelength in width (or an odd multiple, m_{si} & m_{air}), where the wavelength is the centre wavelength of the transmitted pass band (λ_c), in the respective medium ($\lambda_c = 1.55 \mu m$ in air). The middle air-gap cavity is chosen to be half the wavelength (or a multiple, m_{gap}) and the angle θ is assigned to the etching angle caused by the imperfect fabrication process. We assign the notation $m = [m_{si} \ m_{air} \ m_{gap} \ n_{bars}]$ to describe the order of the filter and the number of silicon bars in a mirror, i.e. for our fabricated device $m = [21, 5, 2, 3]$. Using a transfer matrix formulation, one can accurately simulate a 1D air-silicon stack for plane waves, but further investigation is necessary to estimate the effect of non-parallel layers caused by the etching angle, and the angular spectrum resulting from use of fibers. A simple model has been suggested by Wahl [4], but it does not take into account the width of the optical beam and assumes a uniform cavity width throughout the beam. We approximate the incident beam as Gaussian, and expand its plane-wave angular spectrum accordingly. To incorporate the etching angles, we have modelled the system as a wedged Fabry-Perot cavity, with two lossless 1D PBG mirrors on either side. The reflectivity and transmission coefficients of each mirror are calculated using the matrix formulation [5], and are strongly dependant on the incident angle ϕ . The output field can therefore be calculated by tracing the light geometrically as it reflects in the cavity

accumulating angle and phase. This analysis is given in detail in [6].

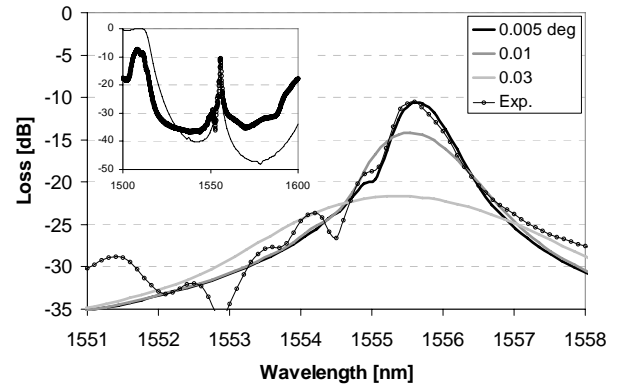


Figure 3: Passband shapes, and full spectra (inset), for various filter etch angles.

Fig. 3 shows a simulated approximation of the effect of the etch angle on the output spectrum. The simulation was carried out for a $9 \mu m$ radius Gaussian beam input and a $m = [21, 5, 2, 3]$ filter. The angle is the taper angle of the silicon features, with $\theta = 0^\circ$ meaning absolutely vertical. It is apparent that the angle tolerance is tight, with a substantial performance degradation at angles larger than 0.005° . The

experimental values are also shown, giving an indication of the precision achieved in the measured device.

3 FABRICATION

To achieve these high fabrication tolerances, we used (110) oriented silicon wafers that have the unique ability to produce vertical trenches when properly aligned to the $\langle 111 \rangle$ flat [7]. Uenishi *et al* have shown that optical devices with high aspect ratios can be fabricated on such wafers, and their atomically flat vertical surfaces were of very high quality, suitable for optical applications such as mirrors and beam splitters [8]. One main drawback to this (110) wet etching technique is that any feature that is not parallel to the (111) planes will be etched in a difficult-to-foresee manner, and though there are several wet etching simulators that aid such designs, it is quite difficult to achieve controlled outcomes. Moreover, since the best practical aspect ratio [9] is $<1:200$, we can conclude that the best etch angle will be $\theta = \tan^{-1}(1/200) = 0.29^\circ$, which is far from sufficient for our needs.

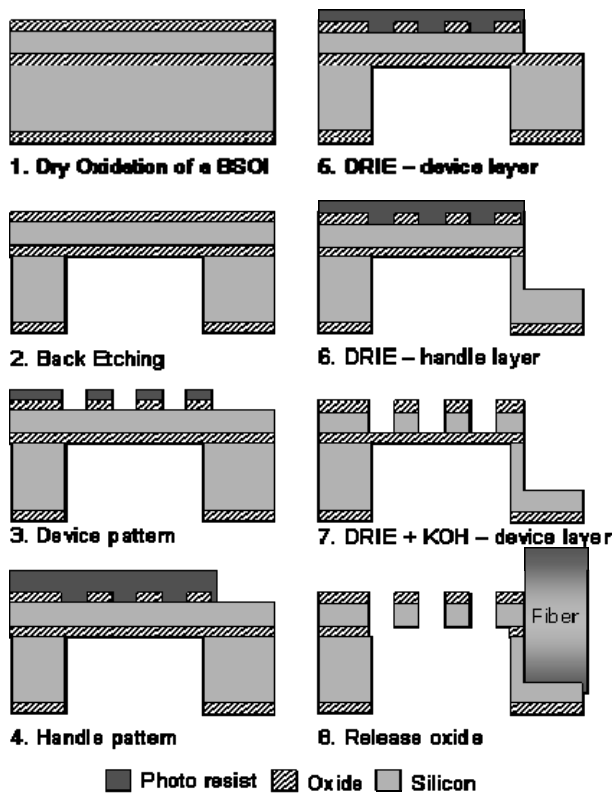


Figure 4: Device fabrication process flow.

To overcome these problems, without losing the benefit of verticality and smoothness, we developed a fabrication process using DRIE for the initial etch, followed by a short KOH wet etching process. This process, illustrated in Fig. 4, is as follows:

1. A Bonded Silicon on Isolator (BSOI) (110) wafer with a $25\mu\text{m}$ device layer and a $0.5\mu\text{m}$ oxide layer is used. A 200nm oxide layer is grown by dry oxidation for masking purposes; 200nm is sufficient for deep etching the $25\mu\text{m}$ device layer.
2. Back etching is used as a release mechanism for the movable parts of the optical filter. Instead of etching the oxide layer with HF and freeze drying to avoid stiction, we create a cavity under the moving part from behind. We find this process to be very reliable with a high yield. The back etching is done at this initial stage, i.e. before creating the filters themselves, to avoid damage to the delicate parts when inverting the wafer. The etch depth is through the entire handle layer, stopping at the oxide layer. The oxide is thick enough to account for the different etching rates of the different sized features.
3. After the back etching, we pattern the top oxide layer with the features of the optical filter parts. A thin S1805 photoresist is used to get a precise pattern transfer, followed by oxide patterning using RIE. It is important to align properly the optical PBG to the $\langle 111 \rangle$ oriented flat in order to achieved vertical surfaces when etched in KOH.
4. The oxide pattern is buried, without etching the silicon, under a thicker resist, which is then patterned to etch the deep grooves needed to integrate the optical fibers.
5. The device layer is etched to create grooves for the optical fibers.
6. The same pattern is used to continue etching through the oxide layer and some of the handle layer. This is needed as the optical fiber half-width is greater than the device layer.
7. Removing the thick resist layer exposes the hidden oxide pattern which is then deep etched. This "hidden mask" process eliminates the need to pattern over an etched surface, which would be inadequate for small features. The DRIE process is followed by the quick KOH etch to smooth and straighten the (111) planes.
8. Oxide is removed from the back to release the structures. No wet processes are allowed, as this breaks the small features.

Fig. 5 shows the released PBG mirrors, with an electrostatic comb-drive actuator on one mirror for tuning the cavity. In this case it proved impossible to implement the KOH step, as the orthogonally oriented comb drive fingers were rapidly destroyed. In Fig. 6 the comb drive is replaced by a simpler actuator consisting of a simple suspension beam which is attracted to the adjacent surface by a differential voltage between them. In this case, the KOH etch could successfully be carried out, and the improved PBG mirror surface quality can be clearly seen. Damage to non-(111) planes is also evident.

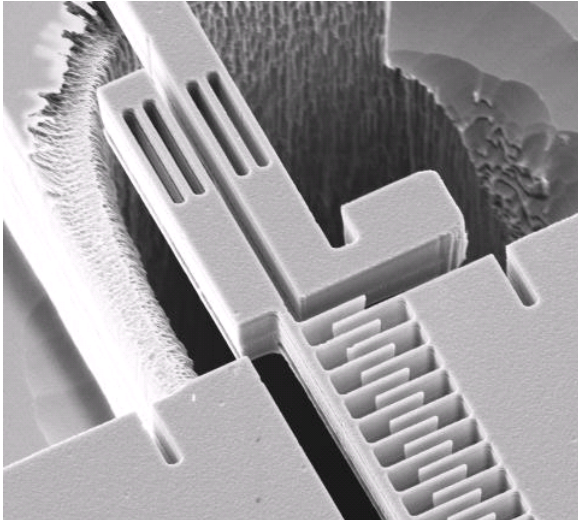


Figure 5: Filter parts and comb drive actuator released by back-etching, but without KOH etching.

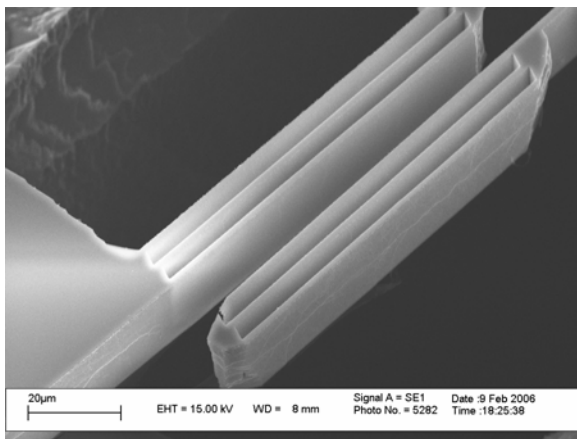


Figure 6: Filter parts released by back-etching, and polished by KOH etching.

4 CONCLUSIONS

In conclusion, a free-space, deep-etched 1D PBG filter has been fabricated and successfully demonstrated. Using a two-step dry etch process, followed by a further anisotropic KOH etch, highly polished and vertical surfaces on the PBG mirrors were obtained. By matching the measured spectrum to a numerical model, an achieved sidewall angle precision of better than 0.01° is estimated. We believe that the use of (110) wafers and KOH etching is essential to receive adequate results for high aspect ratio optical structures of this type. Furthermore, this fabrication approach is promising for other structures where highly parallel surfaces are required. One possibility might be variable capacitors with extremely narrow gaps.

We are grateful to the EPSRC (under the Ultrafast Photonics Consortium) for supporting this work.

REFERENCES

- [1] D. Hohlfield, M. Epmeier, and H. Zappe, "A thermally tunable, silicon-based optical filter," *Sensors and Actuators A (Physical)*, vol. A103, pp. 93-9, 2003.
- [2] C. F. R. Mateus, C.-H. Chang, L. Chrostowski, S. Yang, D. Sun, R. Pathak, and C. J. Chang-Hasnain, "Widely tunable torsional optical filter," *IEEE Photonics Technology Letters*, vol. 14, pp. 819-21, 2002.
- [3] Y. Yi, P. Bermel, K. Wada, X. Duan, J. D. Joannopoulos, and L. C. Kimerling, "Tunable multichannel optical filter based on silicon photonic band gap materials actuation," *Applied Physics Letters*, vol. 81, pp. 4112-14, 2002.
- [4] J. A. Wahl, J. S. Van Delden, and S. Tiwari, "Tapered Fabry-Perot filters," *IEEE Photonics Technology Letters*, vol. 16, pp. 1873-1875, 2004.
- [5] H. A. Macleod, *Thin film Optical Filters*, Third ed: Institute of Physics Publishing, 2002.
- [6] A. Lipson and E. M. Yeatman, "Low-loss one-dimensional photonic bandgap filter in (110) silicon," *Optics letters*, vol. 31, pp. 395-7, 2006.
- [7] D. L. Kendall, "Vertical etching of silicon at very high aspect ratios," in *Annual review of materials science*, vol.9: Annual Reviews Inc, 1979, pp. 373-403.
- [8] Y. Uenishi, M. Tsugai, and M. Mehregany, "Micro-opto-mechanical devices fabricated by anisotropic etching of (110) silicon," *Journal of Micromechanics and Microengineering*, vol. 5, pp. 305-12, 1995.
- [9] A. Holke and H. T. Henderson, "Ultra-deep anisotropic etching of (110) silicon," *Journal of Micromechanics and Microengineering*, vol. 9, pp. 51-7, 1999.
- [10] S.-S. Yun, S.-K. You, and J.-H. Lee, "Fabrication of Vertical Optical Plane using DRIE and KOH Crystalline Etching of (110) Si Wafer," presented at International Conference on Optical MEMS, Takamatsu, Takamatsu, Japan, 2004.